Journal of Science and Technology in Civil Engineering, NUCE 2020. 14 (3): 110–124

EFFECTS OF BENDING STIFFNESS AND SUPPORT EXCITATION OF THE CABLE ON CABLE RAIN-WIND INDUCED INCLINED VIBRATION

Viet-Hung Truong[a,*]

[a]*Faculty of Civil Engineering, Thuyloi University, 175 Tay Son street, Dong Da district, Hanoi, Vietnam*

Article history:
Received 05/06/2020, Revised 10/08/2020, Accepted 11/08/2020

Abstract

The main objective of this paper is to investigate the responses of the inclined cable due to rain-wind induced vibration (RWIV) considering the bending stiffness and support excitation of the cable. The single-degree-of-freedom (SDOF) model is employed to determine the aerodynamic forces. The 3D model of a cable subjected to RWIV is developed using the linear theory of the cable oscillation and the central difference algorithm in which the influences of wind speed change according to the height above the ground, bending stiffness, and support excitation of the cable are considered. The numerical results showed that the cable displacement calculated by considering cable bending stiffness in RWIV is slightly smaller than in the case of neglecting it. And, the cable diameter had a nonlinear relationship with cable displacement, where when both diameter and mass per unit length of cable increase cable displacement will decrease. In addition, the periodic oscillation of cable supports extremely increases the amplitude of RWIV if its frequency is nearby that of the cable.

Keywords: 3D model; inclined cable; rain-wind induced vibration; rivulet; analytical model; vibration.

https://doi.org/10.31814/stce.nuce2020-14(3)-10

1. Introduction

Among the various types of wind-induced vibrations of cables, rain-wind induced vibration (RWIV), first observed by Hikami and Shiraishi [1] on the Meikonishi bridge, has attracted the attention of scientists around the world. Hikami and Shiraishi revealed that neither vortex-induced oscillations nor a wake galloping could explain this phenomenon. After Hikami and Shiraishi, a series of laboratory experiments (Bosdogianni and Olivari [2], Matsumoto et al. [3], Flamand [4], Gu and Du [5], Gu [6]...), and field later (Costa et al. [7], Ni et al. [8]...) were conducted to study this special phenomenon. They found that the basic characteristic of RWIV was the formation of the upper rivulet on cable surface, which oscillated with lower cable modes in a certain range of wind speed under a little or moderate rainfall condition. Furthermore, Wu et al. [9] also observed the amplitude of RWIV was dependent on the length, inclination direction, surface material of the cables, and the wind yaw angle. In other hands, Cosentino et al. [10], Macdonald and Larose [11], Flamand and Boujard [12], and Zuo and Jones [13] indicated that the RWIV was related to Reynolds number and its mechanisms are similar to that of the dry galloping phenomenon of cable. Recently, Du et al. [14] found out that the continuous change of aerodynamic forces acting on the cable owing to the oscillation of the upper rivulet was the excitation mechanics of the RWIV.

*Corresponding author. *E-mail address:* truongviethung@tlu.edu.vn (Truong, V.-H.)

To look into the nature of this phenomenon, lots of theoretical models explaining this phenomenon have been developed. Yamaguchi [15] first established the model with the two-degree-of-freedom theory (2-DOF). He found that when the frequency of upper rivulet oscillation coincided with the cable's natural frequency, aerodynamic damping was negative and caused the large cable displacement. Thereafter, Xu and Wang [16], Wilde and Witkowski [17] presented an SDOF model based on Yamaguchi's theory to aim only to investigate cable response due to RWIV. The forces caused by rivulet oscillation were substituted into the cable vibration equation, considering them as given parameters based on the assumption of rivulets motion law. Gu [6] also developed an analytical model for RWIV of 3D continuous stayed cable with a quasi-steady state assumption. Limaitre et al. [18], based on the lubrication theory, simulated the formation of rivulets and studied the variation of water film around the horizontal and static cable. Bi et al. [19] presented a 2D coupled equations model of water film evolution and cable vibration based on the combination of lubrication and vibration theories of a single-mode system.

Generally, theoretical models so far have been concentrated mainly on the 2D model. According to the knowledge of the author, the number of studies about the 3D model of RWIV of cable was relatively small. Some researches can be listed as Gu [6], Li et al. [20], Li et al. [21], etc. However, these studies were still limited, none being a comprehensive review of the fundamental factors affecting fluctuations of cables, such as the change of inclination angle because of cable sag, the distribution of the rivulet on the entire length of the cable, the effect of cable height. Some important factors that affect the cable vibration also have not been mentioned, such as cable bending stiffness or bridge tower and deck vibration.

To fill this gap in the literature, this paper is to develop the new 3D inclined cable model to investigate the response of the inclined cable due to RWIV considering the bending stiffness and support excitation of the cable. The single-degree-of-freedom model in [16, 17] is applied to calculate the aerodynamic forces. The 3D model of a cable subjected to RWIV is then developed using the linear theory of cable oscillation and the central difference algorithm in which the influences of wind speed change according to the height above the ground, bending stiffness, and support excitation of the cable are considered. The relationship between diameter and RWIV displacement of inclined cable is then investigated. Finally, the effect of cable supports excitation is obtained in RWIV.

2. 3D model of rain – wind induced vibration of the inclined cable

2.1. Aerodynamic forces functions

Based on the single-degree-of-freedom model presented in [16, 17], Truong and Vu [22] developed the functions of the aerodynamic forces as follows:

$$F_{damp} = \frac{D\rho}{2}\left(\begin{array}{l} S_1 + S_2 \sin(\omega t) + S_3 \sin(2\omega t) + S_4 \sin(3\omega t) + S_5 \sin(4\omega t) + \\ S_6 \cos(\omega t) + S_7 \cos(2\omega t) + S_8 \cos(3\omega t) \end{array} \right) \tag{1}$$

$$F_{exc} = \frac{D\rho}{2}\left(\begin{array}{l} X_1 + X_2 \sin(\omega t) + X_3 \sin(2\omega t) + X_4 \sin(3\omega t) + X_5 \sin(4\omega t) + \\ X_6 \cos(\omega t) + X_7 \cos(2\omega t) + X_8 \cos(3\omega t) + X_9 \cos(5\omega t) \end{array} \right) \tag{2}$$

where ρ is the density of the air; D is the diameter of the cable; ω is the cable angular frequency; S_i and X_i are the parameters that can be found in [22]. The oscillation of a cable element is written as

$$\ddot{y} + \left(2\xi_s \omega + \frac{F_{damp}}{m}\right)\dot{y} + \omega^2 y + \frac{F_{exc}}{m} = 0 \tag{3}$$

where ξ_s is the structural damping ratio of the cable; m is the mass of the cable per unit length. Details of the formulation of Eqs. (1) and (2) can be found in [22].

2.2. *The theoretical formulation of the 3D inclined cable model*

Considering an inclined cable in Fig. 1 with the dynamic equilibrium of an element of cable as Fig. 2. Equations governing the motions of a 3D continuous cable in the in-plane motion can be written as

$$\frac{\partial}{\partial s}\left[(T+\Delta T)\left(\frac{dx}{ds}+\frac{\partial u}{\partial s}\right)-(V+\Delta V)\left(\frac{dy}{ds}+\frac{\partial v}{\partial s}\right)\right]+F_x(y,t)=m\frac{\partial^2 u}{\partial t^2}+c\frac{\partial u}{\partial t} \tag{4a}$$

$$\frac{\partial}{\partial s}\left[(T+\Delta T)\left(\frac{dy}{ds}+\frac{\partial v}{\partial s}\right)+(V+\Delta V)\left(\frac{dx}{ds}+\frac{\partial u}{\partial s}\right)\right]+F_y(y,t)=m\frac{\partial^2 v}{\partial t^2}+c\frac{\partial v}{\partial t}-mg \tag{4b}$$

where u and v are the longitudinal and vertical components of the in-plane motion, respectively; T and ΔT are the tension and additional tension generated, respectively; V and ΔV are the shear force and additional shear force, respectively; m and c are the mass per unit length and damping coefficient of the cable, respectively; $F_x(y,t)$ and $F_y(y,t)$ are wind pressure on the cable according to the x and y axes, respectively; g is the gravitational acceleration.

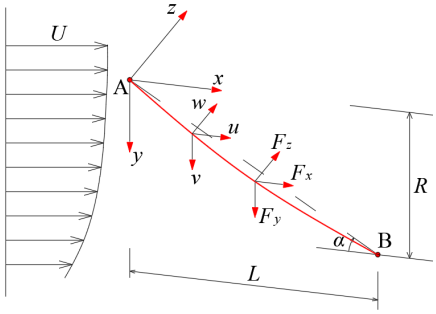

Figure 1. Model of 3D cable

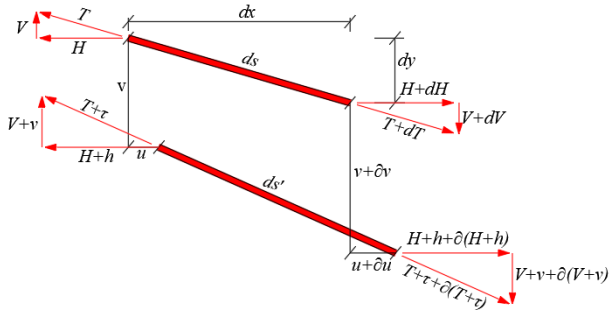

Figure 2. Equilibrium of a cable element

In Fig. 2, the vertical and longitudinal equilibrium of the cable element located at (x, y) require that

$$\frac{d}{ds}\left(T\frac{dy}{ds}\right)=-mg \tag{5a}$$

$$T\frac{dx}{ds}=H \tag{5b}$$

$$\Delta H=\Delta T\frac{dx}{ds} \tag{5c}$$

$$\frac{\partial}{\partial s}=\frac{1}{\sqrt{1+y_x^2}}\frac{\partial}{\partial x} \tag{5d}$$

$$V+\Delta V=\frac{\partial\,(M+\Delta M)}{\partial s}\approx -EI\left(\frac{d^3y}{ds^3}+\frac{d^3v}{ds^3}\right)\approx -EI\frac{d^3v}{ds^3} \tag{5e}$$

where H and ΔH are the horizontal component of cable tension and additional tension, respectively; y_x is the first derivative of the cable equation at the initial position. In Eq. (5e), $\frac{d^3y}{ds^3}$ is eliminated

because the function of cable is assumed quadratic equation of the horizontal coordinate (presented in Eq. (24)).

Substitution of Eqs. (5) into Eqs. (4), and terms of the second-order are neglected. So the equations of motion are transformed into

$$\frac{1}{\sqrt{1+y_x^2}}\frac{\partial}{\partial x}\left[(H+\Delta H)\left(1+\frac{\partial u}{\partial x}\right)\right]+\frac{y_x}{1+y_x^2}EI\frac{\partial^4 v}{\partial x^4}+F_x(y,t)=m\frac{\partial^2 u}{\partial t^2}+c\frac{\partial u}{\partial t} \tag{6a}$$

$$\frac{1}{\sqrt{1+y_x^2}}\frac{\partial}{\partial x}\left[(H+\Delta H)\left(1+\frac{\partial v}{\partial x}\right)+\Delta H y_x\right]-\frac{1}{1+y_x^2}EI\frac{\partial^4 v}{\partial x^4}+F_y(y,t)=m\frac{\partial^2 v}{\partial t^2}+c\frac{\partial v}{\partial t} \tag{6b}$$

2.3. The response of cable to support excitation

The initial condition of two ends of cable: At A: $u_1(t)$ and $v_1(t)$, at B: $u_2(t)$ and $v_2(t)$. The two components of displacement $u(x,t)$ and $v(x,t)$ of a cable subjected at both supports acting in the x and y directions as shown in Fig. 1, are expressed in the form:

$$u(x,t)=u_s(x,t)+u_d(x,t) \tag{7a}$$

$$v(x,t)=v_s(x,t)+v_d(x,t) \tag{7b}$$

where $u_s(x,t)$ and $v_s(x,t)$ are the pseudo-static displacements in the x and y directions, respectively. $u_d(x,t)$ and $v_d(x,t)$ are the relative dynamic displacements in the x and y directions, respectively.

From the geometry of a cable under different support motion [23], the pseudo-static displacements are given by:

$$u_s(x,t)=\left(1-\frac{x}{L}\right)u_1(t)+\frac{x}{L}u_2(t) \tag{8a}$$

$$v_s(x,t)=\left(1-\frac{x}{L}\right)v_1(t)+\frac{x}{L}v_2(t) \tag{8b}$$

Applying Hooke's law and the second order is neglected, we have:

$$\Delta H=\frac{EA}{\left(1+y_x^2\right)^{3/2}}\left(\frac{\partial u}{\partial x}+y_x\frac{\partial v}{\partial x}\right)-\frac{EA}{L_{cab}}(u_1+u_2) \tag{9}$$

where E and A are elastic modulus and cross-sectional area of the cable; L_{cab} is the cable length.

Substitution of Eqs. (7), (8), and (9) into Eqs. (6), consequently Eq. (6) is transformed to

$$\begin{aligned}&\left(a_1\frac{\partial^2 u_d}{\partial x^2}+a_2\frac{\partial^2 v_d}{\partial x^2}+a_3\frac{\partial u_d}{\partial x}+a_4\frac{\partial v_d}{\partial x}\right)+\left(a_3\frac{\partial u_s}{\partial x}+a_4\frac{\partial v_s}{\partial x}\right)+\frac{y_x}{1+y_x^2}EI\frac{\partial^4 v_d}{\partial x^4}-\\&-\frac{1}{\sqrt{1+y_x^2}}\frac{EA}{L_{cab}}(u_1+u_2)\frac{\partial^2 u_d}{\partial x^2}+F_x(y,t)=m\frac{\partial^2 u_d}{\partial t^2}+c\frac{\partial u_d}{\partial t}+m\frac{\partial^2 u_s}{\partial t^2}+c\frac{\partial u_s}{\partial t}\end{aligned} \tag{10a}$$

$$\begin{aligned}&\left(a_5\frac{\partial^2 v_d}{\partial x^2}+a_2\frac{\partial^2 u_d}{\partial x^2}+a_6\frac{\partial v_d}{\partial x}+a_4\frac{\partial u_d}{\partial x}\right)+\left(a_6\frac{\partial v_s}{\partial x}+a_4\frac{\partial u_s}{\partial x}\right)-\frac{1}{1+y_x^2}EI\frac{\partial^4 v_d}{\partial x^4}\\&-\frac{1}{\sqrt{1+y_x^2}}\frac{EA}{L_{cab}}(u_1+u_2)\frac{\partial^2 v_d}{\partial x^2}-\frac{1}{\sqrt{1+y_x^2}}\frac{EA}{L_{cab}}(u_1+u_2)\frac{\partial^2 y}{\partial x^2}+F_y(y,t)\\&=m\frac{\partial^2 v_d}{\partial t^2}+c\frac{\partial v_d}{\partial t}+m\frac{\partial^2 v_s}{\partial t^2}+c\frac{\partial v_s}{\partial t}\end{aligned} \tag{10b}$$

where a_1, a_2, a_3, a_4, a_5, and a_6 are parameters that are given in Appendix A.

2.4. *Discretization of differential equation*

To solve Eqs. (10), the cable is divided into N parts so that the horizontal length of one part is l_h with $l_h = L/N$ (Fig. 3). Using the central difference algorithm for points i from 2 to $N-2$, the components $\frac{\partial^2 u_d}{\partial x^2}$, $\frac{\partial^2 v_d}{\partial x^2}$, and $\frac{\partial^4 v_d}{\partial x^4}$ are estimated as

$$\frac{\partial^2 u_d(x_i)}{\partial x^2} = \frac{1}{l_h^2}\left(u_{d,i-1} - 2u_{d,i} + u_{d,i+1}\right) \tag{11a}$$

$$\frac{\partial^2 v_d(x_i)}{\partial x^2} = \frac{1}{l_h^2}\left(v_{d,i-1} - 2v_{d,i} + v_{d,i+1}\right) \tag{11b}$$

$$\frac{\partial^4 v_d(x_i)}{\partial x^4} = \frac{1}{l_h^4}\left(v_{d,i-2} - 4v_{d,i-1} + 6v_{d,i} - 4v_{d,i+1} + v_{d,i+2}\right) \tag{11c}$$

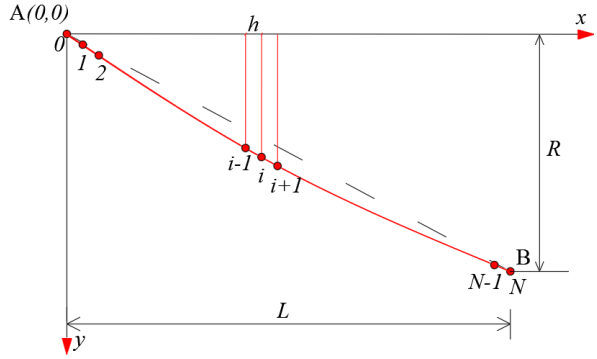

Figure 3. Model of dividing nodes on the cable

At point 1 and point $N-1$:

$$\begin{aligned}
&\frac{\partial^2 u_d(x_1)}{dx^2} = \frac{1}{l_h^2}\left(-2u_{d,1} + u_{d,2}\right) && \frac{\partial^2 v_d(x_1)}{dx^2} = \frac{1}{l_h^2}\left(-2v_{d,1} + v_{d,2}\right)\\
&\frac{\partial^4 u_d(x_1)}{dx^4} = \frac{1}{l_h^4}\left(u_{d,3} - 4u_{d,2} + 7u_{d,1}\right) && \frac{\partial^4 v_d(x_1)}{dx^4} = \frac{1}{l_h^4}\left(v_{d,3} - 4v_{d,2} + 7v_{d,1}\right)\\
&\frac{\partial^2 u_d(x_{n-1})}{dx^2} = \frac{1}{l_h^2}\left(-2u_{d,n-1} + u_{d,n-2}\right) && \frac{\partial^2 v_d(x_{n-1})}{dx^2} = \frac{1}{l_h^2}\left(-2v_{d,n-1} + v_{d,n-2}\right)\\
&\frac{\partial^4 u_d(x_{n-1})}{dx^4} = \frac{1}{l_h^4}\left(u_{d,n-3} - 4u_{d,n-2} + 7u_{d,n-1}\right) && \frac{\partial^4 v_d(x_{n-1})}{dx^4} = \frac{1}{l_h^4}\left(v_{d,n-3} - 4v_{d,n-2} + 7v_{d,n-1}\right)
\end{aligned} \tag{12}$$

Substituting Eqs. (11) and (12) into Eqs. (10), the discrete equations of motion can be obtained as below:

$$[M]\frac{d^2\{u_d\}}{dt^2} + [C]\frac{d\{u_d\}}{dt} + \left([K] + \left[K_{stif}\right] + \left[K_{\sup}(t)\right]\right)\{u_d\} = \{F\} \tag{13}$$

where $[K]$, $[M]$, and $[C]$ given in Appendix A are stiffness, mass, and damping matrix, respectively; $\left[K_{stif}(t)\right]$ and $\left[K_{\sup}(t)\right]$ are the stiffness increases due to bending stiffness and support excitation of cable, respectively; $\{u_d\}$ is the dynamic displacement vector with $\{u_d\} = [u_{d,1}, v_{d,1}, \ldots, u_{d,i}, v_{d,i}, \ldots, u_{d,N-1}, v_{d,N-1}]^T$, and $\{F\}$ is force vector with $\{F\} = \left[F_x(y_1,t), F_y(y_1,t), \ldots, F_x(y_{N-1},t), F_y(y_{N-1},t)\right]^T$.

According to Section 2.1, the aerodynamic forces acting on the cable element i^{th} are written as

$$F_{damp}(i) = F_{damp}(U(i), \gamma_0(i), \alpha(i), \theta_0(i), a_m(i), t) \tag{14a}$$

$$F_{exc}(i) = F_{exc}(U(i), \gamma_0(i), \alpha(i), \theta_0(i), a_m(i), t) \tag{14b}$$

As can be seen in Eqs. (14), aerodynamic forces include two components F_{exc} and F_{damp}, in which F_{damp} continuously changes the damping ratio of oscillation. Thus, the damping matrix $[C]$ and force vector $\{F\}$ in Eq. (13) are rewritten as

$$[DAMP] = [C] + \left[F_{damp}\right] \tag{15}$$

$$\{F\} = \{F_{exc}\} + \{F_{sta}\} + \{F_{sta1}\} + \{F_{sta2}\} \tag{16}$$

where $[DAMP]$, $\left[F_{damp}\right]$, $\{F_{\text{exc}}\}$,$\{F_{sta}\}$, $\{F_{sta1}\}$, and $\{F_{sta2}\}$ are given in Appendix A. Now, Eq. (13) can be expressed as

$$[M]\frac{d^2\{u_d\}}{dt^2} + [DAMP]\frac{d\{u_d\}}{dt} + \left([K] + \left[K_{stif}\right] + \left[K_{\text{sup}}(t)\right]\right)\{u_d\} = \{F_{\text{exc}}\} \tag{17}$$

The total displacements at nodes can be calculated as follows. From Eqs. (8) the vector of pseudo-static displacements is given by

$$\{u_s\} = \{u_{1,s}, v_{1,s}, \ldots, u_{i,s}, v_{i,s}, \ldots, u_{N-1,s}, v_{N-1,s}\}^T \tag{18}$$

in which:

$$u_{i,s}(t) = (1-i)u_1(t) + iu_2(t) \tag{19a}$$

$$v_{i,s}(t) = (1-i)v_1(t) + iv_2(t) \tag{19b}$$

The vector of total displacements as follows:

$$\{u\} = \{u_s\} + \{u_d\} \tag{20}$$

The change of wind velocity according to the height above the ground can be calculated by using the below equation [24]:

$$\frac{U_0(y_1,t)}{U_0(y_2,t)} = \left(\frac{y_1}{y_2}\right)^n \tag{21}$$

where $U_0(y_1,t)$ and $U_0(y_2,t)$ are wind velocities at the heights y_1 and y_2, respectively; n is an empirically derived coefficient that is dependent on the stability of the atmosphere. For neutral stability conditions, n is approximately 1/7, or 0.143. Therefore, n is assumed to be equal to 0.143 in this study. The unstable balance angle, θ_0, and the amplitude, a_m, of the rivulet on the cable surface can be calculated as follows [24]:

$$\theta_0 = 0.0525U_0^3 - 1.75U_0^2 + 14.72U_0 + 24.938 \text{ for } 6.5 < U_0 < 12.5(\text{m/s}) \tag{22}$$

$$a_m = -1.9455U_0^4 + 60.543U_0^3 - 699.05U_0^2 + 3557U_0 - 6738.4 \text{ for } 6.5 < U_0 \leq 9.5(\text{m/s}) \tag{23a}$$

$$a_m = -2.1667U_0^4 + 97.167U_0^3 - 1626.2U_0^2 + 12028U_0 - 33137 \text{ for } 9.5 < U_0 < 12.5(\text{m/s}) \tag{23b}$$

$$a_m = 0 \text{ for } U_0 \leq 6.5 \text{ or } 12.5 \leq U_0 \tag{23c}$$

The function of cable shape is assumed as a quadratic equation of the horizontal coordinate as

$$y = -\frac{mg}{2H}\sec(\alpha)\,x^2 + \frac{mgL}{2H}\sec(\alpha)\,x + \tan(\alpha)\,x \tag{24}$$

Matrix of inclination angle $\{\alpha\}$ with

$$\tan(\alpha(i)) = \frac{mg}{H}\sec(\alpha)\,x(i) \tag{25}$$

Matrix of the effective wind speed $\{U\}$ and wind angle effect $\{\gamma_0\}$ in the cable plane is

$$U(i) = U_0(i)\sqrt{\cos^2\beta + \sin^2\alpha(i)\sin^2\beta} \tag{26}$$

where $\{U_0\}$ is the matrix of initial wind velocity calculated from Eq. (21), and

$$\gamma_0(i) = \sin^{-1}\left(\frac{\sin\alpha(i)\sin\beta}{\sqrt{\cos^2\beta + \sin^2\alpha(i)\sin^2\beta}}\right) \tag{27}$$

Finally, we have the formula of aerodynamic forces at the node i^{th} as

$$F_{damp}(i) = F_{damp}(U(i), \gamma_0(i), \alpha(i), \theta_0(i), a_m(i), t) \tag{28a}$$
$$F_{exc}(i) = F_{exc}(U(i), \gamma_0(i), \alpha(i), \theta_0(i), a_m(i), t) \tag{28b}$$

3. Results and discussion

The investigated cable has the following properties: length $L_{cab} = 330.4$ m, mass per unit length $m = 81.167$ kg/m, diameter $D = 0.114$ m, first natural frequency $f = 0.42$ Hz, structural damping ratio $\xi_s = 0.1\%$. RWIV appears in the range of wind velocity from 6.5 m/s to 12.5 m/s, and maximum amplitude peaks at 9.5 m/s. The initial conditions are $y_0 = 0.001$ m and $\dot{y}_0 = 0$. The inclination and the yaw angles are 27.80 and 350, respectively. The coefficients C_D and C_L are calculated based on the actual angle between the wind acting on cable and the rivulet, ϕ_e, as follows [24]:

$$C_D = -1.6082\phi_e^3 - 2.4429\phi_e^2 - 0.5065\phi_e + 0.9338 \tag{29a}$$
$$C_L = 1.3532\phi_e^3 + 1.8524\phi_e^2 + 0.1829\phi_e - 0.0073 \tag{29b}$$

The cable is divided into 20 elements to perform the above-developed analysis.

3.1. Influence of cable bending stiffness on RWIV

Eq. (17) is developed based on the general evaluation of many factors that influence the RWIV of the inclined cable, especially bending stiffness and supports excitation of cable. In this section, the influence of cable bending stiffness on RWIV is considered. Notes that, the simple model without considering bending stiffness and supports excitation of cable can be found in [24]. In this cable model, Eq. (17) is rewritten as follows:

$$[M]\frac{d^2\{u\}}{dt^2} + [DAMP]\frac{d\{u\}}{dt} + \left([K] + \left[K_{stif}\right]\right)\{u\} = \{F_{exc}\} \tag{30}$$

Eq. (30) shows that matrix $\left[K_{stif}(t)\right]$ is the change of cable rigidity due to its bending stiffness. Clearly, the bigger ratio between two matrixes $\left[K_{stif}(t)\right]$ and $[K]$ is, the larger the effects of cable bending are. From Eqs. (A.9) and (A.10), diameter and length of cable are the parameters that greatly influence the value of the matrix$\left[K_{stif}(t)\right]$. To obtain effects of cable bending stiffness in RWIV, six cases of diameter (D) are analyzed corresponding to $0.5D$, $0.8D$, D, $1.2D$, $1.5D$, and $2D$. Notes that, mass per unit length (m) closely relates with diameter. However, to deeply understand the effect of cable bending stiffness on RWIV, such as (1) m is changed according to D, and (2) m is constant.

Figs. 4 and 5 show the maximum cable displacement according to wind velocity with different cable diameters. With initial values of cable diameter, the maximum cable displacements are 33.27 and 33.126 cm corresponding to the cable model ignoring and considering cable bending stiffness, respectively. It also can be seen that the shape of cable responses according to wind velocity is identical in all the cases. Cable amplitude increases from the wind speed of 5.5 m/s to 9.5 m/s and then decreases up to 12.5 m/s. With each wind velocity, cable displacement is proportional to the diameter if mass per unit length is constant. This is in contrast to the case that diameter and mass per unit length of cable change together.

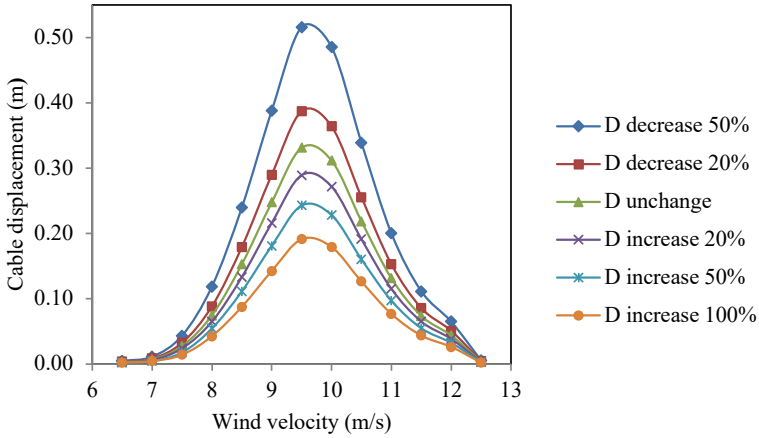

(a) No considering cable bending stiffness

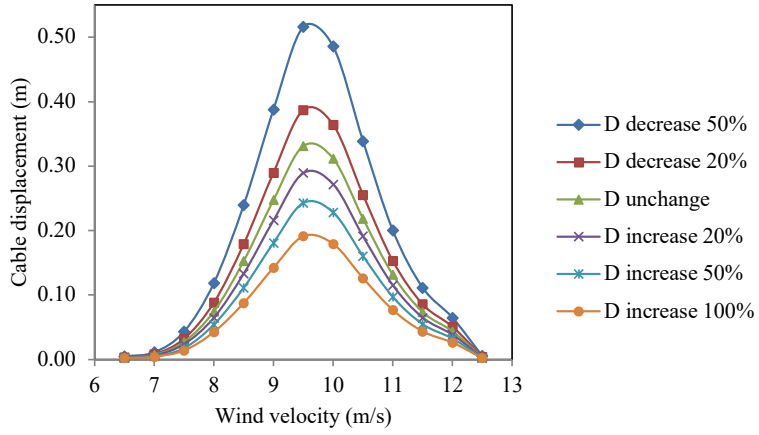

(b) Considering cable bending stiffness

Figure 4. Cable response with the variation of cable diameter and mass per length

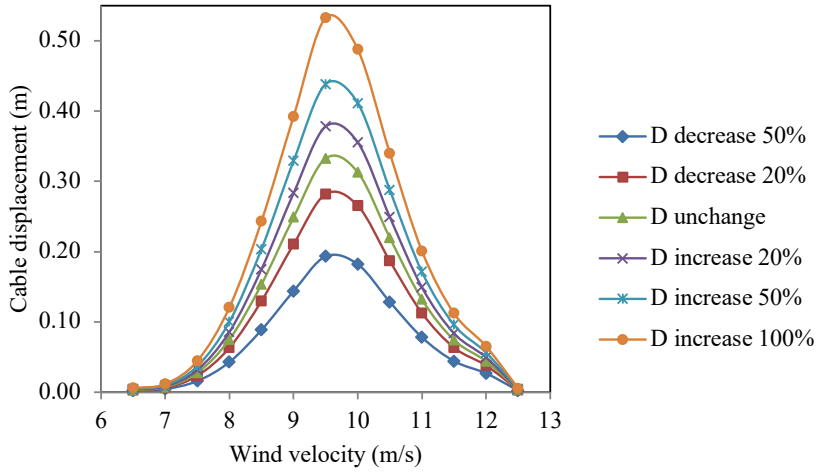

(a) No considering cable bending stiffness

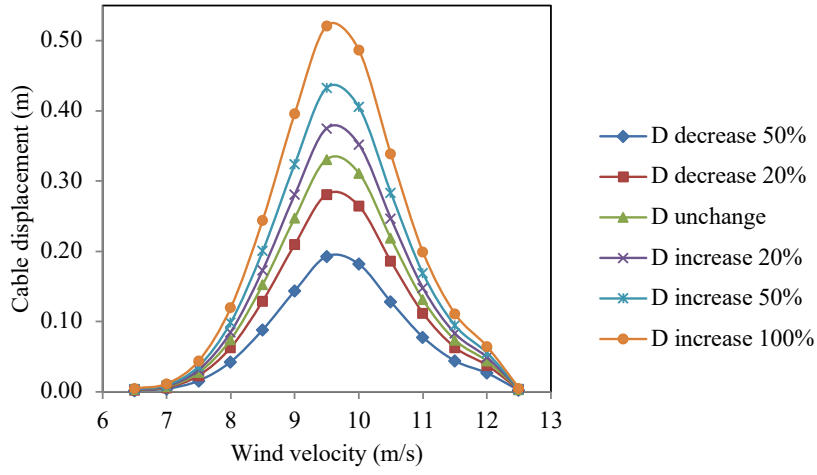

(b) Considering cable bending stiffness

Figure 5. Cable response with the variation of cable diameter

Fig. 6 and Table 1 show cable displacement at wind velocity 9.5 m/s with different cable diameters. Four case studies are calculated corresponding to the considering and neglecting cable bending stiffness in the RWIV model combining with m changing and not changing according to D. For simplicity, the results are presented in the form of the ratio with those of the initially investigated cable where the cable bending stiffness is ignored. As can be seen in Fig. 6, if mass per unit length and diameter of cable change together, the maximum cable displacement decreases when cable diameter increases. Specifically, when cable diameter rises 300%, the cable displacement drops about 57.51% and 58.52% corresponding to the cable model considering or ignoring cable bending stiffness. If mass per unit length of the cable is constant when cable diameter changes, contrary to the first case, the cable maximum displacement is proportional to cable diameter. For example, the cable displacement increases about 160.17% and 156.72% corresponding to the cable model considering and ignoring cable bending stiffness when cable diameter rises 200%. Furthermore, in all cases, the curve lines in Fig. 6 indicate that the relationship between cable displacement and cable diameter is nonlinear and the change of cable displacement reduces when cable diameter continues to increase.

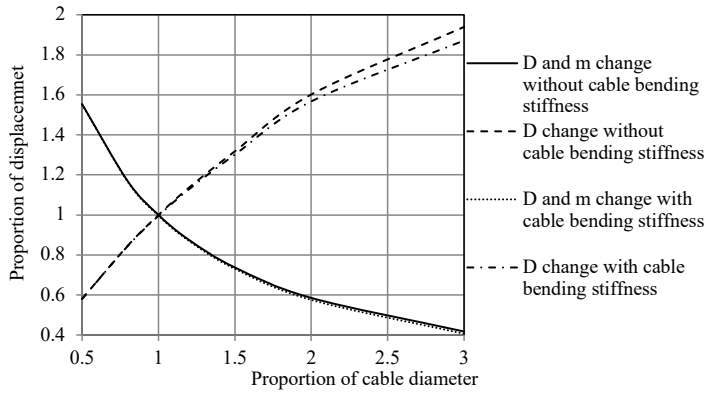

Figure 6. Change of cable displacement with different cable diameter (U_0 = 9.5 m/s)

Table 1. Comparison of cable responses with cable bending stiffness (U_0 = 9.5 m/s)

Change of cable diameter (%)	The case *m* and *D* change			The case only *D* change		
	No considering cable bending stiffness	Considering cable bending stiffness	Rate (%)	No considering cable bending stiffness	Considering cable bending stiffness	Rate (%)
50	0.51680	0.51622	−0.1121	0.19318	0.19306	−0.0665
80	0.38827	0.38724	−0.2664	0.28190	0.28131	−0.2086
100	0.33272	0.33126	−0.4403	0.33272	0.33126	−0.4403
120	0.29107	0.28937	−0.5829	0.37817	0.37539	−0.7354
150	0.24533	0.24292	−0.9817	0.43848	0.43298	−1.2551
200	0.19471	0.19136	−1.7214	0.53293	0.52146	−2.1524
300	0.13886	0.13507	−2.7297	0.64525	0.62261	−3.5082

On the other hand, it is easy to recognize that the cable bending stiffness reduces cable displacement in RWIV. The ratio of cable amplitude reduction is shown in Fig. 6 combined with Fig. 7. When the diameter *D* is 0.114 m, the decline is about 0.4403%. This value increases quickly from 0.4403% to more than 2.7% when the diameter *D* rises 300%. However, there is a big difference in the reduc-

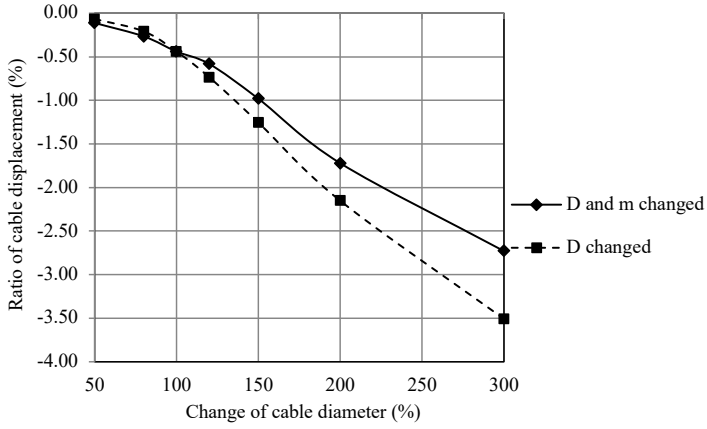

Figure 7. Cable amplitude reduction with different cable diameter

tion of cable amplitude in two cases of the diameter change. In Fig. 7, the cable amplitude reduction in the case that both D and m increase is smaller than the case that only D increases, and vice versa.

3.2. Influence of periodic excitation of cable supports on RWIV

In a cable-stayed bridge, inclined cables connecting the pylons and the deck by anchorages have different lengths. Thus, the cable oscillation is naturally associated with wind- or traffic-induced vibration of the deck and/or the towers. If the frequency of oscillation of the deck and/or towers falls in certain ranges, the stay cables may be excited and exhibit large response amplitudes. It should be noted that the interactive movements of deck and pylon are very complex and need deeper structural analysis. To easily obtain the effects of excitation of cable supports on RWIV, the vibration of anchorages is assumed to be periodic, and only deck vibration is considered. RWIV of inclined cable is studied with harmonic vertical excitation of its lower support as follows:

$$v_2(t) = v_2 \sin(\omega_1 t) \tag{31}$$

where v_2 and ω_1 are the amplitude and the angular frequency of vertical excitation of the cable lower support. The cable model considering cable bending stiffness in Section 3.1 continues to be studied. Three cases of v_2 are analyzed corresponding to 1 cm, 2 cm, and 3 cm.

Fig. 8 shows the cable displacement with different values of ω_1. Obviously, cable amplitude is very large when the value of ω_1 is nearly angle frequency of RWIV of the cable ω. The cable displacement is 1.13 m, 2.59 m, and 4.06 m corresponding to ω_1 is 1 cm, 2 cm, and 3 cm. These values are too greater than cable displacement of RWIV of cable (33.126 cm). However, when the ratio ω_1/ω is smaller 95% or larger 105%, the effect of support periodic vibration is small. With ω_1/ω = 95%, cable displacement is 37.83 cm, 42.7 cm, and 47.59 cm corresponding to ω_1 is 1 cm, 2 cm, and 3 cm. This means that the displacement of RWIV of cable increases by about 14.2%, 28.91%, and 43.68%, respectively. Clearly, deck oscillation with a small amplitude makes a large displacement of RWIV of cable.

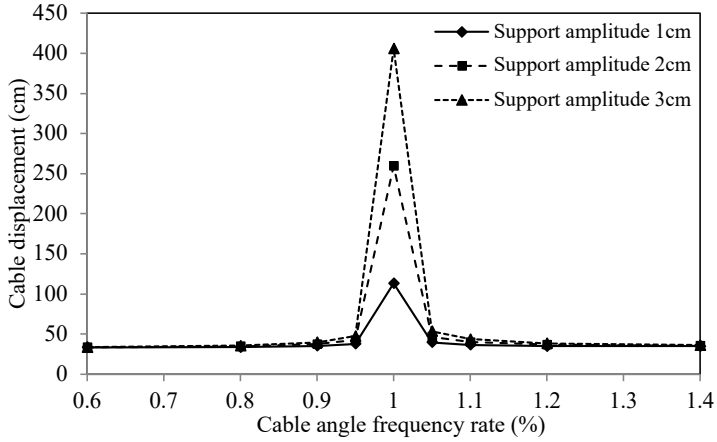

Figure 8. Cable displacement with different angle frequency of cable lower support vibration

4. Conclusions

The new 3D model considering the bending stiffness and support excitation of the cable was successfully developed for RWIV of the inclined cable. The following points can be summarized

from the present study:

- The cable bending stiffness reduces cable displacement in RWIV but not great. This effect is proportional to cable diameter. In the case of cable study in this paper, the displacement of cable RWIV decreases about 2.7 – 3.7% when cable diameter increases by 300%.

- The cable diameter had a nonlinear relationship with cable displacement. This relationship is proportional if only cable diameter changes. When both diameter and mass per unit length of cable increase, cable displacement will decrease.

- The periodic oscillation of cable supports extremely affects RWIV of the inclined cable when its frequency is nearby that of cable. In other cases, its effect is still quite significant.

References

[1] Hikami, Y., Shiraishi, N. (1988). Rain-wind induced vibrations of cables in cable stayed bridges. *Journal of Wind Engineering and Industrial Aerodynamics*, 29:409–418.

[2] Bosdogianni, A., Olivari, D. (1996). Wind-and rain-induced oscillations of cables of stayed bridges. *Journal of Wind Engineering and Industrial Aerodynamics*, 64(2-3):171–185.

[3] Matsumoto, M., Shiraishi, N., Shirato, H. (1992). Rain-wind induced vibration of cables of cable-stayed bridges. *Journal of Wind Engineering and Industrial Aerodynamics*, 43(1-3):2011–2022.

[4] Flamand, O. (1995). Rain-wind induced vibration of cables. *Journal of Wind Engineering and Industrial Aerodynamics*, 57(2-3):353–362.

[5] Gu, M., Du, X. (2005). Experimental investigation of rain–wind-induced vibration of cables in cable-stayed bridges and its mitigation. *Journal of wind engineering and industrial aerodynamics*, 93(1):79–95.

[6] Gu, M. (2009). On wind–rain induced vibration of cables of cable-stayed bridges based on quasi-steady assumption. *Journal of Wind Engineering and Industrial Aerodynamics*, 97(7-8):381–391.

[7] Costa, A. P. d., Martins, J. A. C., Branco, F., Lilien, J.-L. (1996). Oscillations of bridge stay cables induced by periodic motions of deck and/or towers. *Journal of Engineering Mechanics*, 122(7):613–622.

[8] Ni, Y. Q., Wang, X. Y., Chen, Z. Q., Ko, J. M. (2007). Field observations of rain-wind-induced cable vibration in cable-stayed Dongting Lake Bridge. *Journal of Wind Engineering and Industrial Aerodynamics*, 95(5):303–328.

[9] Wu, T., Kareem, A., Li, S. (2013). On the excitation mechanisms of rain–wind induced vibration of cables: Unsteady and hysteretic nonlinear features. *Journal of Wind Engineering and Industrial Aerodynamics*, 122:83–95.

[10] Cosentino, N., Flamand, O., Ceccoli, C. (2003). Rain-wind induced vibration of inclined stay cables–Part I: Experimental investigation and physical explanation. *Wind and Structures*, 6(6):471–484.

[11] Macdonald, J. H. G., Larose, G. L. (2008). Two-degree-of-freedom inclined cable galloping–Part 2: Analysis and prevention for arbitrary frequency ratio. *Journal of wind Engineering and industrial Aerodynamics*, 96(3):308–326.

[12] Flamand, O., Boujard, O. (2009). A comparison between dry cylinder galloping and rain-wind induced excitation. In *Proceeding of the 5th European & African Conference on Wind Engineering*, Florence, Italy.

[13] Zuo, D., Jones, N. P. (2010). Interpretation of field observations of wind-and rain-wind-induced stay cable vibrations. *Journal of Wind Engineering and Industrial Aerodynamics*, 98(2):73–87.

[14] Du, X., Gu, M., Chen, S. (2013). Aerodynamic characteristics of an inclined and yawed circular cylinder with artificial rivulet. *Journal of Fluids and Structures*, 43:64–82.

[15] Yamaguchi, H. (1990). Analytical study on growth mechanism of rain vibration of cables. *Journal of Wind Engineering and Industrial Aerodynamics*, 33(1-2):73–80.

[16] Xu, Y. L., Wang, L. Y. (2003). Analytical study of wind–rain-induced cable vibration: SDOF model. *Journal of Wind Engineering and Industrial Aerodynamics*, 91(1-2):27–40.

[17] Wilde, K., Witkowski, W. (2003). Simple model of rain-wind-induced vibrations of stayed cables. *Journal of Wind Engineering and Industrial Aerodynamics*, 91(7):873–891.

[18] Lemaitre, C., Hémon, P., de Langre, E. (2007). Thin water film around a cable subject to wind. *Journal of Wind Engineering and Industrial Aerodynamics*, 95(9-11):1259–1271.

[19] Bi, J. H., Wang, J., Shao, Q., Lu, P., Guan, J., Li, Q. B. (2013). 2D numerical analysis on evolution of water film and cable vibration response subject to wind and rain. *Journal of Wind Engineering and Industrial Aerodynamics*, 121:49–59.

[20] Li, S. Y., Gu, M., Chen, Z. Q. (2007). Analytical model for rain–wind-induced vibration of three-dimensional continuous stay cable with quasi-moving rivulet. *Engineering Mechanics*, 24(6):7–12.

[21] Li, S. Y., Gu, M., Chen, Z. Q. (2009). An analytical model for rain-wind-induced vibration of three-dimentional continuous stay cable with actual moving rivulet. *Journal of Human University (Natural Sciences)*, 36:1–7. (in Chinese).

[22] Hung, T. V., Viet, V. Q. (2019). A 2D model for analysis of rain-wind induced vibration of stay cables. *Journal of Science and Technology in Civil Engineering (STCE)-NUCE*, 13(2):33–47.

[23] Rao, G. V., Iyengar, R. N. (1991). Seismic response of a long span cable. *Earthquake Engineering & Structural Dynamics*, 20(3):243–258.

[24] Hung, T. V., Viet, V. Q., Anh, V. Q. (2020). A three-dimensional model for rain-wind induced vibration of stay cables in cable-stayed bridges. *Journal of Science and Technology in Civil Engineering (STCE)-NUCE*, 14(1):89–102.

Appendix A.

$$[M] = m\,[I] \tag{A.1}$$

$$[C] = c\,[I] \tag{A.2}$$

$$a_1 = \frac{H}{\sqrt{1+y_x^2}} + \frac{EA}{\left(1+y_x^2\right)^2} \tag{A.3}$$

$$a_2 = \frac{EAy_x}{\left(1+y_x^2\right)^2} \tag{A.4}$$

$$a_3 = -\frac{3EAy_x}{\left(1+y_x^2\right)^3}\frac{\partial^2 y}{\partial x^2} \tag{A.5}$$

$$a_4 = \frac{EA\left(1-2y_x^2\right)}{\left(1+y_x^2\right)^3}\frac{\partial^2 y}{\partial x^2} \tag{A.6}$$

$$a_5 = \frac{H}{\sqrt{1+y_x^2}} + \frac{EAy_x^2}{\left(1+y_x^2\right)^2} \tag{A.7}$$

$$a_6 = \frac{EA\left(2y_x - y_x^3\right)}{\left(1+y_x^2\right)^3}\frac{\partial^2 y}{\partial x^2} \tag{A.8}$$

$$a_7 = \frac{y_x}{1+y_x^2}\frac{EI}{l_h^4} \tag{A.9}$$

$$a_8 = -\frac{1}{1+y_x^2}\frac{EI}{l_h^4} \tag{A.10}$$

$$a_9 = a_3\frac{-u_1(t)+u_2(t)}{L} + a_4\frac{-v_1(t)+v_2(t)}{L} \tag{A.11}$$

$$a_{10} = a_4\frac{-u_1(t)+u_2(t)}{L} + a_6\frac{-v_1(t)+v_2(t)}{L} \tag{A.12}$$

$$a_{11}(t) = -\frac{u_1(t)+u_2(t)}{\sqrt{1+y_x^2}}\frac{EA}{l_h^2 L_{cab}} \tag{A.13}$$

$$a_{12}(t) = -\frac{u_1(t)+u_2(t)}{\sqrt{1+y_x^2}}\frac{EA}{L_{cab}}\frac{\partial^2 y}{\partial x^2} \tag{A.14}$$

$$[A_i] = \begin{bmatrix} \frac{a_1(i)}{{l_h}^2} - \frac{a_3(i)}{2l_h} & \frac{a_2(i)}{{l_h}^2} - \frac{a_4(i)}{2l_h} \\ \frac{a_2(i)}{{l_h}^2} - \frac{a_4(i)}{2l_h} & \frac{a_5(i)}{{l_h}^2} - \frac{a_6(i)}{2l_h} \end{bmatrix} \tag{A.15}$$

$$[B_i] = \begin{bmatrix} -\frac{2a_1(i)}{{l_h}^2} & -\frac{2a_2(i)}{{l_h}^2} \\ -\frac{2a_2(i)}{{l_h}^2} & -\frac{2a_5(i)}{{l_h}^2} \end{bmatrix} \tag{A.16}$$

$$[C_i] = \begin{bmatrix} \frac{a_1(i)}{{l_h}^2} + \frac{a_3(i)}{2l_h} & \frac{a_2(i)}{{l_h}^2} + \frac{a_4(i)}{2l_h} \\ \frac{a_2(i)}{{l_h}^2} + \frac{a_4(i)}{2l_h} & \frac{a_5(i)}{{l_h}^2} + \frac{a_6(i)}{2l_h} \end{bmatrix} \tag{A.17}$$

$$K = -\begin{bmatrix} [B_1] & [C_1] & & & & & & & \\ [A_2] & [B_2] & [C_2] & & & & & & \\ & & \cdots & \cdots & & & & & \\ & & & [A_i] & [B_i] & [C_i] & & & \\ & & & & \cdots & \cdots & & & \\ & & & & [A_{N-2}] & [B_{N-2}] & [C_{N-2}] & & \\ & & & & & [B_{N-1}] & [C_{N-1}] & & \end{bmatrix} \tag{A.18}$$

$$\left[A_{stif,i}\right] = \begin{bmatrix} 0 & 6a_7(i) \\ 0 & 6a_8(i) \end{bmatrix} \tag{A.19}$$

$$\left[B_{stif,i}\right] = \begin{bmatrix} 0 & -4a_7(i) \\ 0 & -4a_8(i) \end{bmatrix} \tag{A.20}$$

$$\left[C_{stif,i}\right] = \begin{bmatrix} 0 & a_7(i) \\ 0 & a_8(i) \end{bmatrix} \tag{A.21}$$

$$\left[D_{stif}\right] = \begin{bmatrix} 0 & 7a_7(1) \\ 0 & 7a_8(1) \end{bmatrix} \tag{A.22}$$

$$K_{stif} = -\begin{bmatrix} [D_{stif}] & [B_{stif,1}] & [C_{stif,1}] & & & & & & & & \\ [B_{stif,2}] & [A_{stif,2}] & [B_{stif,2}] & [C_{stif,2}] & & & & & & & \\ [C_{stif,3}] & [B_{stif,3}] & [A_{stif,3}] & [B_{stif,3}] & [C_{stif,3}] & & & & & & \\ \cdots & \cdots & \cdots & \cdots & \cdots & \cdots & \cdots & \cdots & \cdots & \cdots \\ & & & & & [C_{stif,n-3}] & [B_{stif,n-3}] & [A_{stif,n-3}] & [B_{stif,n-3}] & [C_{stif,n-3}] \\ & & & & & & [C_{stif,n-2}] & [B_{stif,n-2}] & [A_{stif,n-2}] & [B_{stif,n-2}] \\ & & & & & & & [C_{stif,n-1}] & [B_{stif,n-1}] & [D_{stif}] \end{bmatrix} \tag{A.23}$$

$$\left[A_{\mathrm{sup},i}\right] = \begin{bmatrix} 0 & a_{11}(i,t) \\ 0 & a_{11}(i,t) \end{bmatrix} \tag{A.24}$$

$$\left[B_{\mathrm{sup},i}\right] = \begin{bmatrix} 0 & -2a_{11}(i,t) \\ 0 & -2a_{11}(i,t) \end{bmatrix} \tag{A.25}$$

$$K_{\mathrm{sup}}(t) = -\begin{bmatrix} [B_{\mathrm{sup},1}(t)] & [A_{\mathrm{sup},1}(t)] & & & & & & \\ [A_{\mathrm{sup},2}(t)] & [B_{\mathrm{sup},2}(t)] & [A_{\mathrm{sup},2}(t)] & & & & & \\ \cdots & \cdots & \cdots & \cdots & \cdots & \cdots & \cdots & \\ & & [A_{\mathrm{sup},i}(t)] & [B_{\mathrm{sup},i}(t)] & [A_{\mathrm{sup},i}(t)] & & & \\ \cdots & \cdots & \cdots & \cdots & \cdots & \cdots & \cdots & \\ & & & & [A_{\mathrm{sup},n-2}(t)] & [B_{\mathrm{sup},n-2}(t)] & [A_{\mathrm{sup},n-2}(t)] & \\ & & & & & [A_{\mathrm{sup},n-1}(t)] & [B_{\mathrm{sup},n-1}(t)] & \end{bmatrix} \tag{A.26}$$

$$\left[F_{damp}\right] = \begin{bmatrix} F_{x,damp}(y_1,t) & & & & & & \\ & F_{y,damp}(y_1,t) & & & & & \\ & & \cdots & & & & \\ & & & F_{x,damp}(y_{N-1},t) & & & \\ & & & & F_{y,damp}(y_{N-1},t) & & \end{bmatrix} \tag{A.27}$$

$$\{F_{exc}\} = \left[F_{x,exc}(y_1,t), F_{y,exc}(y_1,t), \ldots, F_{x,exc}(y_{N-1},t), F_{y,exc}(y_{N-1},t)\right]^T \tag{A.28}$$

$$\{F_{sta}\} = [a_9(1,t), a_{10}(1,t), a_9(2,t), a_{10}(2,t), \ldots, a_9(N-1,t), a_{10}(N-1,t)]^T \tag{A.29}$$

$$F_{sta1,u}(i,t) = -\left\{m\left[\left(1-\frac{i}{n}\right)\frac{\partial^2 u_1(t)}{\partial t^2} + \frac{i}{n}\frac{\partial^2 u_2(t)}{\partial t^2}\right] + c\left[\left(1-\frac{i}{n}\right)\frac{\partial u_1(t)}{\partial t} + \frac{i}{n}\frac{\partial u_2(t)}{\partial t}\right]\right\} \tag{A.30}$$

$$F_{sta1,v}(i,t) = -\left\{m\left[\left(1-\frac{i}{n}\right)\frac{\partial^2 v_1(t)}{\partial t^2} + \frac{i}{n}\frac{\partial^2 v_2(t)}{\partial t^2}\right] + c\left[\left(1-\frac{i}{n}\right)\frac{\partial v_1(t)}{\partial t} + \frac{i}{n}\frac{\partial v_2(t)}{\partial t}\right]\right\} \tag{A.31}$$

$$\{F_{sta1}\} = [F_{sta1,u}(1,t), F_{sta1,v}(1,t), F_{sta1,u}(2,t), F_{sta1,v}(2,t), \ldots, F_{sta1,u}(N-1,t), F_{sta1,v}(N-1,t)]^T \tag{A.32}$$

$$\{F_{sta2}\} = [0, a_{12}(1,t), 0, a_{12}(2,t), \ldots, 0, a_{12}(N-1,t)]^T \tag{A.33}$$